Biogeochemistry (2015) 123:329–347
DOI 10.1007/s10533-015-0085-4

Spatial and temporal variability in carbon dioxide and methane exchange at three coastal marshes along a salinity gradient in a northern Gulf of Mexico estuary

Benjamin J. Wilson · Behzad Mortazavi · Ronald P. Kiene

Received: 18 March 2014 / Accepted: 15 September 2014 / Published online: 27 February 2015

Abstract Carbon gas fluxes in tidal marshes vary spatially and temporally because of vegetation cover, subsurface biogeochemical processes, and environmental forcing. The objective of this study was to examine how ecosystem carbon gas exchange changes along an estuarine salinity gradient. We measured carbon dioxide (CO_2) and methane (CH_4) gas fluxes from three marshes representing a salinity gradient (0–32 ppt) in the Mobile Bay estuary, Alabama, USA. CH_4 flux was relatively small with no significant differences across sites despite salinity differences. Interestingly, sediment porewater CH_4 concentrations were significantly higher at the high salinity salt marsh and decreased with decreasing salinity. Midday net ecosystem exchange (where a positive rate indicates net carbon assimilated through photosynthesis) was greatest at the most fresh site (4.8 ± 0.3 μmol CO_2 m^{-2} s^{-1}), followed by the saline (2.8 ± 1.0 μmol CO_2 m^{-2} s^{-1}) and brackish (1.4 ± 0.6 μmol CO_2 m^{-2} s^{-1}) sites. However, net ecosystem exchange integrated diurnally revealed each marsh to be a net CO_2 source to the atmosphere as a result of high ecosystem respiration with the freshwater marsh emitting more CO_2 (-893.4 ± 187.9 g C m^{-2} $year^{-1}$) than the brackish (-517.8 ± 85.2 g C m^{-2} $year^{-1}$) and salt marsh (-410.2 ± 98.2 g C m^{-2} $year^{-1}$). This finding leads to the conclusion that either the marshes are losing carbon or that they receive a subsidy of respirable carbon, possibly via tidal deposition. The extent to which sedimentation from tidal deposition contributes carbon to these ecosystems, however, remains unknown. Without such a subsidy, marshes in the study area will not be able to keep up with sea level rise.

Keywords Carbon dioxide · Methane · Climate change · Primary production · Ecosystem respiration · Mobile Bay Alabama

Responsible Editor: Torben Christensen.

B. J. Wilson (✉) · B. Mortazavi
Department of Biological Sciences, University of Alabama, Box 870344, Tuscaloosa, AL 35487, USA
e-mail: bwils034@fiu.edu; benwilso@fiu.edu

B. J. Wilson · B. Mortazavi · R. P. Kiene
Dauphin Island Sea Lab, 101 Bienville Boulevard, Dauphin Island, AL 36528, USA

Present Address:
B. J. Wilson
Department of Biological Sciences, Florida International University, Miami, FL 33199, USA

R. P. Kiene
Department of Marine Sciences, University of South Alabama, Mobile, AL 36688, USA

Introduction

Rising atmospheric carbon dioxide (CO_2) and methane (CH_4) concentrations have stimulated interest in studying carbon (C) cycling between terrestrial

ecosystems and the atmosphere. Wetlands, in particular, are important to the global C cycle because of their large C pools and ability to sequester C via peat formation, sediment deposition, and plant biomass accumulation (Bridgham et al. 2006; Page et al. 2011), yet freshwater wetlands are an important source of the potent greenhouse gas CH_4 (Bastviken et al. 2011; Whalen 2005). Conversely, saline wetlands are relatively small CH_4 sources compared to their freshwater counterparts (Poffenbarger et al. 2011). Although coastal wetlands account for only ~0.3–5 % of the earth's total wetlands, they typically store 100–300 g C m^{-2} $year^{-1}$, which is up to 50 times more C than any other terrestrial ecosystem (Chmura et al. 2003; Duarte et al. 2005; McLeod et al. 2011; Reddy and DeLaune 2008). However, the maintenance of this sequestered C pool is uncertain given anthropogenic influences and future changes in climate (Kirwan and Megonigal 2013).

A warming climate, resulting from increased greenhouse gas emissions, is causing a gradual but substantial increase in the rate of sea level rise (SLR) (IPCC 2007). Increased rates of SLR will cause saltwater to intrude on historically freshwater tidal marshes, which in turn can cause a significant change in C cycling dynamics (Neubauer 2013; Weston et al. 2006). Changes in C accumulation rates can determine whether or not a marsh is able to keep pace with SLR. The ability of coastal marshes to act as C sinks depends on the balance between primary production and export of C as respiration products (i.e. CO_2 and CH_4) and detritus (Inglett et al. 2012; McLatchey and Reddy 1998). Variations in salinity affect both primary production and sedimentary biogeochemical processes (Bartlett et al. 1987; Delaune et al. 1983a). Changes in salinity can drive shifts in vegetation regimes (Perry and Hershner 1999; Schuyler et al. 1993) and change photosynthetic efficiencies and growth rates of marsh vegetation (Neubauer 2013; Pezeshki et al. 1987). Increases in salinity generally leads to an increase in sulfate (SO_4^{2-}) concentrations, which can shift belowground microbial communities and ecosystem respiration as competition for electron donors leads to a switch in microbial respiratory pathways (Neubauer et al. 2005; Weston et al. 2006, 2011). Although a variety of studies of coastal wetlands have attempted to explain some of the variations in C fluxes from a single marsh (Chmura et al. 2011; Magenheimer et al. 1996; Neubauer 2013), few have looked at how these dynamics of both CO_2 and CH_4 fluxes differ with changing salinity (Weston et al. 2014).

To investigate rates of C exchange from the northern Gulf of Mexico's coastal marshes, we conducted a 1-year field study (January 2012 to January 2013) at three sites with contrasting salinity and vegetative covers. Our objective was to provide an assessment of CO_2 and CH_4 fluxes from marshes with differing salinities and examine how differing site characteristics influenced these fluxes. We hypothesized that hydrogen sulfide (H_2S) would increase across the salinity gradient from fresh to salt marsh as saltwater will enhance microbial sulfate reduction. Gross ecosystem exchange (GEE) would decrease along this same gradient as increases in porewater ion concentrations (e.g. H_2S, Cl^-, SO_4^{2-}) would reduce the productivity and growth of plants (Koch et al. 1990). Ecosystem respiration of CO_2 (ER_{CO2}) would also decrease as GEE and ER_{CO2} are tightly linked (Cannell and Thornley 2000). We also hypothesized that there would be a reduction in CH_4 emissions along the salinity gradient from freshwater to salt marsh as increased SO_4^{2-} concentrations would inhibit CH_4 production. In addition to testing the above hypotheses, we used ecosystem respiration and air temperature data to estimate the potential increase in CO_2 efflux that could result from future climatic warming. Results from this study add to our knowledge of how C cycling in coastal marshes may change with saltwater intrusion resulting from SLR and with climate warming.

Methods

Study sites

The study sites were located at three diurnal intertidal marshes within the Mobile Bay estuary, Alabama (Fig. 1). Week's Bay (30°26.56′N, 87°48.52′W) is characterized as a tidal freshwater marsh dominated by *Cladium jamaicense* and is only flooded on spring high tides or during easterly wind events. Dog River (30°35.13′N, 88°07.05′W) is a brackish marsh dominated by *C. jamaicense* and floods only on spring high tides. The salt marsh ecosystems on Dauphin Island (30°15.43′N, 88°07.438′W) are dominated by

Fig. 1 Study site locations within the Mobile Bay Estuary, Alabama, USA

Spartina alterniflora interspersed with *Juncus roemerianus* and are flooded on every high tide.

Carbon flux measurements

Three permanent aluminum collars at each site were embedded 10 cm into the sediment in December 2011 and provided an airtight seal between the marsh and the chamber. Each collar had twelve 2.5-cm diameter holes positioned at the sediment surface to allow for natural flooding and drainage. Ecosystem exchanges of CO_2 and CH_4 were measured with transparent, temperature-regulated static chambers (0.26 m^2 × 1.02 m tall), modified from Neubauer et al. (2000), that enclosed both marsh plants and sediments. The chamber was equipped with three 4.8 m^3 min^{-1} fans that circulated air within the chamber. A thermocouple inside the chamber recorded air temperature, and, in order to keep internal chamber temperature within 2 °C of ambient temperature, a temperature controller regulated a pump that circulated ice water through a heat exchanger when chamber temperatures increased ≥0.5 °C above ambient. During C flux measurements, incident irradiance was measured every minute with a quantum light sensor (Apogee Instruments, Logan, UT, USA model MQ-200) placed adjacent to the plots. Concurrently, a thermometer measured soil temperature at 10 cm depth. Gas flux measurements were made during low or neap tides monthly between January 2012 and January 2013 and were taken within 2 h of solar noon on sunny days, when possible. Preliminary measurements conducted during December 2011 showed that vegetation at each site needed only 2 min to equilibrate and produce linear changes in CO_2 concentrations over time. Prior to taking flux measurements, drainage holes were sealed, the chamber was placed into a lip in the collar and sealed with water, and the entire system was allowed to equilibrate for 5 min.

CO_2 fluxes

During flux measurements, air was pumped from the chamber to a calibrated CO_2 gas analyzer (LI-COR. Lincoln, NE, USA model LI-820) placed in line with the chamber. In order to determine how NEE of CO_2 would vary over a daily solar cycle, and to develop photosynthesis versus irradiance relationships, NEE flux measurements were made for 4–5 min at 100, 52, 47, and 12 % maximum sun light intensity (chamber covered with shade cloth), and in the dark. From August 2012 until the end of the study period, the 47 % shade cloth treatment was eliminated because of similarities to the 52 % density shade cloth and time constraints. CO_2 concentrations were measured every 5 s at each light level. In between sampling at each light level, the chamber was removed from the collar and allowed to equilibrate with atmospheric conditions. The chamber was then placed back in the collar, covered with the appropriate shade cloth, and allowed to equilibrate for 2 min before flux measurements were started. A full cycle of measurements on a single plot took roughly 40 min. Plot "C" at Week's Bay during July 2012 was not sampled as a result of equipment failure. NEE was measured in full light and intermediated light levels while ecosystem respiration of CO_2 (ER_{CO2}) was measured in the dark. GEE was calculated from NEE and ER_{CO2} as:

$$GEE = NEE - ER_{CO2}, \quad (1)$$

where NEE was instantaneous CO_2 flux into the marsh ($\mu mol\ m^{-2}\ s^{-1}$) in light and ER_{CO2} was the CO_2 flux out of the marsh in the dark. A negative NEE indicates that the marsh is a net source of CO_2 to the atmosphere, while a positive NEE corresponds to a net CO_2 sink.

CH_4 fluxes

CH_4 efflux was measured in the dark immediately following CO_2 measurements. To determine the linearity of CH_4 fluxes, triplicate air samples were removed from the chamber of one plot at each site every 10–15 min for 40 min, stored in 40 mL evacuated glass serum vials (Wheaton, Millville, NJ, USA), and analyzed with a flame ionization detector on a Shimadzu GC-2014 gas chromatograph (Shimadzu Scientific Instruments, Columbia, MD, USA). CH_4 fluxes from the other two plots were measured by extracting an air sample in triplicate at the beginning (0 min) and end (40 min) and analyzed as described above. A needle piercing a second septa kept the pressure inside the chamber at equilibrium with the atmosphere (Delaune et al. 1983a). Gas fluxes were calculated as the change in concentration over time (Vourlitis et al. 1993). For most sampling events, C flux measurements were taken at all three sites within a 3–5 day period.

Porewater analyses

Concurrent with gas flux measurements, porewater salinity and nutrient measurements were made from porewater sippers equipped with a 5-cm sampling window of porous plastic (Porex, 25–40 μm pore size). Each experimental plot contained two sippers, one each at 10 and 25 cm depth (Neubauer 2013). Before sampling, the sippers were purged of water and flushed with N_2 gas, keeping conditions anoxic. After roughly 30 min, triplicate porewater samples were withdrawn with a syringe, filtered, and placed into 15 mL plastic centrifuge tubes. Samples were kept on ice until returned to the lab where they were frozen until analysis. PO_4^{3-}, NH_4^+, NO_2^-, and NO_3^- concentrations were analyzed with an automated wet chemistry analyzer–continuous flow analyzer (San Plus System, Skalar Analytical, The Netherlands). Porewater SO_4^{2-}/Cl^- ratios from all sippers were measured with an ion chromatograph (Dx-120, Dionex, Sunnyvale, CA) and were used to calculate SO_4^{2-} depletion (SD):

$$SD = [Cl^-] \times 0.0517 - [SO_4^{2-}], \quad (2)$$

where $[Cl^-]$ and $[SO_4^{2-}]$ are the measured chloride and SO_4^{2-} concentrations and 0.0517 is the ratio of SO_4^{2-} to chloride in seawater (Hsieh and Yang 1997). Porewater salinity was calculated as:

$$Salinity(ppt) = 0.0018066 \times [Cl^-], \quad (3)$$

where $[Cl^-]$ is the chloride concentration in mg/L.

Separate porewater samples were collected to measure H_2S concentrations. 5 mL of porewater was withdrawn and placed into a 12 mL gas-tight Exetainer tubes (Labco, Ceredigion, UK) containing 50 μL of zinc acetate (0.05 M) to preserve the sample. Samples were stored in the dark until analysis. H_2S concentrations were determined colorimetrically (Fonselius 1976). Absorbance was measured with a spectrophotometer at 670 nm (HP 8453, Hewlett-Packard, Palo Alto, CA).

Porewater CH_4 concentrations down to 25 cm were measured from three random cores extracted from each of the marshes. Each core was subsampled at 0, 8, 15, and 25 cm depth. Subsamples (0.5 mL) were placed into a 40-mL glass serum vial, sealed with a gastight stopper and crimp cap, and put on ice until they could be sterilized (1 h in a boiling water bath) in the lab. After cooling to room temperature, samples were vortexed for 2 min to allow the CH_4 in the porewaters to come to equilibrium before they were analyzed on a gas chromatograph. Water content of each individual sediment sample used for CH_4 analysis was determined by weight loss after drying at 70 °C for 48 h. Methane concentrations were normalized to volume of porewater for each sample.

Vegetation biomass

Vegetative belowground biomass was quantified seasonally at each site during May, August, October 2012, and January 2013. Two randomly spaced cores were taken with a 5-cm diameter corer down to 20 cm depth and sectioned at 5-cm intervals. Each sediment sample was stored and frozen until analysis. Separation of roots from sediments and detritus was performed by running a jet of water over the samples

and sieving over soil screens (Symbula and Day 1988). The sieves had 2 and 0.25-mm pore openings. Roots were removed from the sieve with a small stream of water or forceps where necessary. All the roots were then dried at 70 °C and weighed.

Aboveground biomass samples were harvested at the end of the experiment in January 2013. All vegetation in all three plots at each site was clipped at the sediment surface and separated based on vitality. The vegetation was then dried at 70 °C and weighed.

Carbon flux integrations

GEE was integrated over each month from short-term CO_2 fluxes and local meteorological data (irradiance and air temperature; after Neubauer et al. 2000) obtained from a National Oceanic and Atmospheric Administration National Estuarine Research Reserve System (NOAA-NERRS) weather station located at Week's Bay, within ~33 km of all study sites. GEE flux measured in the field was used to generate GEE versus irradiance (GEE vs. PAR) curves for each individual plot measured during the sampling period (Fig. 2a). Hyperbolic curves were fit to GEE versus PAR for each monthly sampling period according to:

$$\mathrm{GEE} = [(a \times I)/(b + I)], \quad (4)$$

where GEE was total photosynthetic uptake (μmol CO2 m^{-2} s^{-1}), I was incident irradiance (μmol m^{-2} s^{-1}), and a and b were empirically derived constants (Whiting et al. 1992). Best-fit regressions for the constants a and b were derived for each plot on a monthly basis using curve-fitting routine in Sigmaplot (v. 12.0, Systat Software Inc., San Jose, CA). Monthly GEE was calculated by taking irradiance data averaged over 15 min time intervals (NOAA-NERRS, 2012) and integrating the results over a period in which PAR was above 10 μmol m^{-2} s^{-1} to obtain a monthly gross photosynthetic uptake rate.

CO_2 fluxes taken in the dark from all sampling months combined were regressed against air temperature. The data was fitted to exponential curves using curve-fitting routine in SigmaPlot:

$$\mathrm{ER_{CO2}} = Ae^{B \times T}, \quad (5)$$

where $\mathrm{ER_{CO2}}$ was the ecosystem respiration of CO_2 rate (μmol C m^{-2} s^{-1}), T was air temperature (°C), and A and B were empirically derived constants

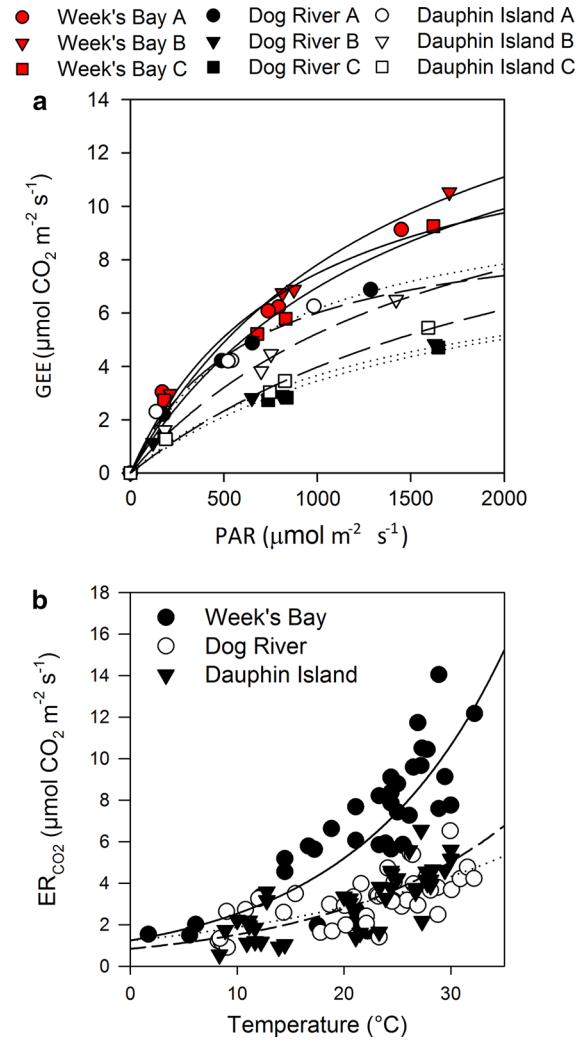

Fig. 2 **a** Light response curves created for 3 plots per site every month at different light intensities were used to determine how gross ecosystem exchange (GEE) would vary over a diurnal solar cycle. This example from March 2012 shows strong correlation at each site despite small variability. Week's Bay had the highest GEE response to PAR (*solid lines*), while Dog River (*dotted lines*) and Dauphin Island (*dashed lines*) showed similar, lower responses. Similar curves were created each month of the study period and were used to integrate GEE over a diurnal cycle. **b** Relationship between temperature and ecosystem respiration of CO_2 ($\mathrm{ER_{CO2}}$) for the entire study period. These curves were used to integrate $\mathrm{ER_{CO2}}$ over a diurnal cycle each month

(Miller et al. 2001). The curves allowed for the extrapolation of CO_2 respiration rates to temperatures encountered during the sampling year. One $\mathrm{ER_{CO2}}$ versus T relationship was created for each site (Fig. 2b). These environmental relationships were

then combined with air temperature data measured every 15 min (NOAA-NERRS, 2012) to estimate monthly ER_{CO2}. Similarly, monthly-integrated NEE was calculated every 15 min from GEE and ER_{CO2} rates.

Warming simulation

A warming simulation was performed in order to examine how much ER_{CO2} would increase in a warmer climate. Two different global temperature scenarios (2 and 4 °C increase) were used in accordance with predicted scenarios by 2100 (IPCC 2007). The same air temperature data described above was subjected to a 2 and a 4 °C temperature increase and inputted into Eq. 5 to estimate ER_{CO2}.

Statistical analyses

Midday NEE, ER_{CO2}, and ER_{CH4} rates were analyzed as a repeated measures analysis in SAS (v.9.3; SAS Institute Inc., Cary, North Carolina) using SAS procedure PROC MIXED. Because plots were measured over time, time was included as a random effect to account for the repeated measures nature of the data. Fixed effects were plot and site. Normality and homoscedasticity were tested by visually inspecting plotted residuals. CH_4 flux data was log transformed in all cases in order to increase homoscedasticity when investigating possible effects. Possible effects investigated were soil temperature, porewater Cl^- (salinity), surface water salinity, CH_4, H_2S, SO_4^{2-}, PO_4^{3-}, NH_4^+, NO_3^-, and NO_2^- porewater concentrations, PAR, NEE, and ER_{CO2}. Depth-specific and temporal differences in porewater salinity, nutrients, and H_2S concentrations were assessed with a standard least squares ANOVA, with date and depth as model effects. Differences in CH_4 emissions, NEE, ER_{CO2}, and GEE flux across sites was analyzed using a repeated measures ANOVA with site specific differences determined using a Holm-Sidak multiple comparison or Tukey's HSD.

Results

Site characteristics

Total aboveground biomass at Week's Bay (820 ± 344 g m^{-2}) and Dog River (751 ± 299 g m^{-2}) was much higher than Dauphin Island (280 ± 84 g m^{-2}) (Table 1). Live aboveground biomass was greater at Week's Bay (454 ± 135 g m^{-2}) than at Dog River (290 ± 165 g m^{-2}) and Dauphin Island (129 ± 54 g m^{-2}). Dead aboveground biomass accounted for 44, 61, and 54 % of the total aboveground biomass at Week's Bay, Dog River, and Dauphin Island, respectively. Belowground biomass did not vary across sites ($F_{(2,9)} = 0.26$, $p = 0.780$) but did vary seasonally. Belowground biomass was greater during the summer months (May and August) than the winter months (October and January) at both Week's Bay ($F_{(1,30)} = 8.0$, $p = 0.008$) and Dog River ($F_{(1,30)} = 4.7$, $p = 0.038$), yet there was no difference between seasons at Dauphin Island ($F_{(1,30)} = 0.01$, $p = 0.911$). Porewater Cl^-, SO_4^{2-}, NH_4^+, and PO_4^{3-} were similar at Week's Bay and Dog River but all significantly higher at Dauphin Island (Table 2).

Environmental conditions

Average daily midday air temperatures during the study period ranged from 8.9 (February 2012) to 30.8 °C (June 2012). Soil temperatures at 10 cm (Fig. 3a) ranged from a low of 8.5 °C (February 2012) to a high of 30.6 °C (August 2012) and were not different across sites ($F_{(2,12)} = 2.5$, $p = 0.104$). Surface water salinity across sites was different throughout the entire study period (Fig. 3b, c; $F_{(2,12)} = 153.1$, $p < 0.001$). Week's Bay was the freshest site with an average salinity of 2.3 ppt with Dog River (4.7 ppt), and Dauphin Island (20.7 ppt), being progressively more saline. Porewater salinities at Week's Bay were lower for the entire study period compared to Dog River ($t = 3.33$, $p = 0.004$). However, surface water salinity at Week's Bay and Dog River were only marginally significantly different ($t = 2.12$, $p = 0.045$), as surface water salinity was much more variable than porewater salinity.

Midday carbon flux measurements

Rates of ecosystem CH_4 emission ranged from undetectable (all sites, January 2012) to 0.07 μmol CH_4 m^{-2} s^{-1} (Week's Bay, August 2012, Fig. 4). CH_4 fluxes over the study period were highly variable and were unexpectedly not correlated to soil temperature (Table 3). For example, maximum flux at Week's Bay in March 2012 was 0.06 μmol CH_4

Table 1 Characterization of above and below-ground vegetation at each study site

Site	Vegetation type	LAB (g m^{-2})	DAB (g m^{-2})	BB (g m^{-3})
Week's Bay	*Cladium jamaicense*	453.6 ± 135.4	366.7 ± 212.0	254.0 ± 121.5
Dog River	*Cladium jamaicense*	290.0 ± 164.5	460.5 ± 138.6	286.1 ± 128.1
Dauphin Island	*Spartina alterniflora*	129.0 ± 54.4	151.0 ± 31.8	275.9 ± 56.3

Live aboveground biomass (LAB) and dead aboveground biomass (DAB) is the total dry weight per unit area of all vegetation collected from each plot within a site and separated by vitality ($n = 3$). Belowground biomass (BB) is the averaged dry weight of 2 cores at each site down to 20 cm averaged over the entire study period. Errors indicate ± one standard deviation

Table 2 Porewater concentrations of chloride (Cl^-), sulfate (SO_4^{2-}), nitrate and nitrite (NO_X), ammonium (NH_4^+), and phosphate (PO_4^{3-}) measured seasonally over the study period for three sites along the salinity gradient

Date	Cl^- (μM)	SO_4^{2-} (μM)	NO_X (μM)	NH_4^+ (μM)	PO_4^{3-} (μM)
Week's Bay					
May 2012	31.7 ± 3.8	5.0 ± 2.0	0.9 ± 0.3	6.0 ± 1.5	0.2 ± 0.2
August 2012	45.7 ± 4.9	1.2 ± 0.3	0.8 ± 0.1	12.6 ± 8.9	0.1 ± 0.0
October 2012	57.4 ± 5.8	1.5 ± 0.1	0.7 ± 0.3	22.1 ± 25.8	0.9 ± 1.3
January 2013	91.4 ± 5.1	6.3 ± 1.0	26.1 ± 40.0	33.7 ± 25.2	1.5 ± 1.7
Average	56.6 ± 8.9	3.5 ± 2.1	8.7 ± 20.0	18.6 ± 30.1	0.7 ± 1.6
Rank	A	A		A	A
Dog River					
May 2012	59.4 ± 6.8	2.3 ± 0.3	0.1 ± 0.1	34.1 ± 7.4	1.1 ± 0.2
August 2012	57.4 ± 8.8	0.8 ± 0.1	0.3 ± 0.1	73.3 ± 23.0	1.3 ± 0.2
October 2012	59.4 ± 4.2	1.2 ± 0.4	0.2 ± 0.1	94.4 ± 50.3	1.7 ± 0.5
January 2013	86.8 ± 26.8	5.2 ± 1.5	1.6 ± 0.3	51.5 ± 29.6	1.8 ± 1.1
Average	65.8 ± 17.9	2.4 ± 0.9	0.6 ± 0.2	63.3 ± 57.7	1.5 ± 0.8
Rank	A	A		A	A
Dauphin Island					
May 2012	346.9 ± 8.5	13.9 ± 0.9	BD	101.8 ± 19.2	5.4 ± 3.4
August 2012	379.8 ± 9.9	16.6 ± 1.4	0.5 ± 0.1	189.4 ± 36.9	3.5 ± 1.7
October 2012	379.5 ± 6.2	18.3 ± 3.7	0.2 ± 0.1	259.8 ± 29.6	2.0 ± 3.1
January 2013	367.1 ± 31.7	17.9 ± 2.7	2.5 ± 2.3	180.0 ± 30.1	7.7 ± 0.9
Average	368.3 ± 21.4	16.7 ± 4.3	1.1 ± 1.2	182.8 ± 52.2	4.7 ± 4.9
Rank	B	B		B	B
F	1446.29	319.725	1.629	28.118	32.47
p	<0.001	<0.001	0.21	<0.001	<0.001

Concentrations represent the average (± SD) of three cores ($n = 3$) with measurements taken at 10 and 25 cm depth. Rank denotes significant difference across sites, where different letters indicates a difference between the two sites (Tukey's post hoc; $p < 0.05$) based on repeated measures analysis ($F_{(2,3)}$ and p values given)

m^{-2} s^{-1}, but declined to 0.01 μmol CH_4 m^{-2} s^{-1} in April and May 2012. Surprisingly, CH_4 fluxes varied little between the three sites, only being significantly different for five out of the thirteen months studied ($F_{(2,46)} = 7.9$, $p < 0.05$). During the summer (May to September) when temperatures were at their highest and respiration rates were maximal, no difference in the magnitude of fluxes was seen across the salinity gradient ($F_{(2,4)} = 3.6$, $p = 0.077$). Mean daily CH_4 emissions from Week's Bay, Dog River, and Dauphin Island were 28.8 ± 9.6, 14.4 ± 8.4, and 15.6 ± 2.4 mg C m^{-2} day^{-1}, respectively.

Across the 13-month sampling period, seasonal patterns of CO_2 flux changed with salinity. Midday NEE measured at solar noon exhibited a pattern of C uptake or neutrality throughout the study period (Fig. 5). Noontime NEE rates were highest at Week's Bay (9.5 ± 0.9 μmol CO_2 m^{-2} s^{-1}, April 2012) and lowest at Dog River (−0.4 ± 0.6 μmol CO_2 m^{-2} s^{-1}, July 2012). Midday NEE averaged over the study year

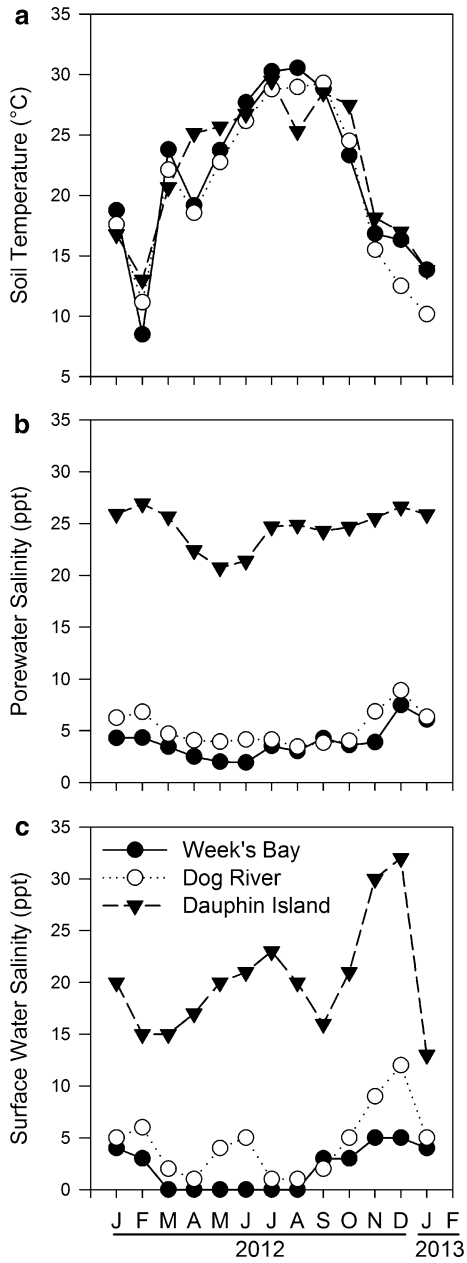

Fig. 3 Soil temperature (**a**) porewater salinity (**b**) and surface water salinity (**c**) plotted for the entire study period (January 2012 to January 2013). Soil temperatures were measured at 10 cm depth in the sediments, porewater salinity was calculated from chloride ion concentrations at 10 cm depth, and surface water salinity was measured with a hand-held refractometer in the field

was greatest at Week's Bay (4.8 ± 0.3 μmol CO_2 m^{-2} s^{-1}) followed by Dauphin Island and Dog River (2.8 ± 1.0 vs. 1.4 ± 0.6 μmol CO_2 m^{-2} s^{-1}, respectively). Throughout the study period, NEE was

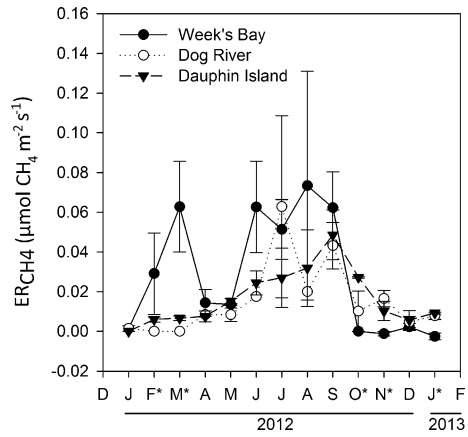

Fig. 4 Short-term ecosystem respiration (ER) of CH_4 from 3 replicate plots at each site. *Error bars* indicate ± 1 SD

greatest at Week's Bay ($F_{(24,69)} = 4.35$, $p < 0.001$), while NEE was slightly greater at Dauphin Island compared to Dog River (Holm-Sidak, $t = 2.26$, $p = 0.033$).

ER_{CO2} was low and nearly identical across all sites through the winter months (January and February 2012), but increased dramatically at Week's Bay at the beginning of the growing season (March 2012) (Fig. 5). ER_{CO2} ranged from 1.0 μmol CO_2 m^{-2} s^{-1} (mean for Dauphin Island, February 2012) to 12.2 μmol CO_2 m^{-2} s^{-1} (Week's Bay, July 2012). Throughout most of the study period, ER_{CO2} was highest at Week's Bay compared to the other two sites ($F_{(24,70)} = 8.63$, $p < 0.001$), and there was no difference in ER_{CO2} rates between Dog River and Dauphin Island ($p = 0.910$, Fig. 5). For all sites, ER_{CO2} was strongly correlated to soil ($F_{(21,29)} = 2.37$, $p = 0.016$) and air temperature ($F_{(21,29)} = 2.02$, $p = 0.040$, Table 3). Q_{10} coefficients, the proportional change in respiration rate with a 10°C change in temperature, were 2.1, 1.5, and 1.8 for Week's Bay, Dog River, and Dauphin Island, respectively.

Calculated GEE at solar noon ranged from 2.4 μmol CO_2 m^{-2} s^{-1} (mean for Week's Bay, January 2012) to 17.9 μmol CO_2 m^{-2} s^{-1} (Week's Bay, May 2012, Fig. 5). GEE was different across all sites ($F_{(24,69)} = 6.09$, $p < 0.001$) with the exception of January and February 2012. During the study period, peak GEE was greater at Week's Bay (Holm-Sidak, $t = 7.32$, $p < 0.001$), while rates at Dog River and Dauphin Island were generally similar ($t = 1.41$,

Table 3 *F*-statistic, numerator degrees of freedom (nDoF), denominator degrees of freedom (dDoF), *p* value, and *r* correlation, when significant, from a repeated measures mixed model ANOVA investigating potential correlation factors on CH_4 emissions, ecosystem respiration of CO_2 (ER_{CO2}), and net ecosystem exchange (NEE)

Potential correlation factor	CH_4					ER_{CO2}					NEE				
	F statistic	nDoF	dDoF	*p*-value	*r*	*F* statistic	nDoF	dDoF	*p*-value	*r*	*F* statistic	nDoF	dDoF	*p*-value	*r*
Soil temperature	3.81	17	13	0.217		2.37	21	29	**0.016**	0.551	2.18	20	27	**0.029**	−0.004
Air temperature	2.22	18	14	0.068		2.02	21	29	**0.040**	0.516	2.17	21	28	**0.028**	0.061
Porewater H_2S	1.51	17	11	0.247		1.16	20	25	0.361		0.70	20	24	0.785	
Porewater CH_4	1.67	19	13	0.174		0.39	21	29	0.985		1.04	21	28	0.456	
Porewater $NO_2^- + NO_3^-$	2.81	11	14	**0.036**	−0.338	0.53	18	28	0.919		0.69	19	28	0.802	
Porewater SO_4^{2-}	1.44	19	13	0.253		0.60	21	29	0.882		0.49	21	28	0.950	
Porewater Cl^-	1.26	19	13	0.342		0.85	21	29	0.649		1.38	21	28	0.211	
Porewater PO_4^{3-}	0.93	17	13	0.564		0.72	19	27	0.770		0.60	20	27	0.880	
ER_{CO2}	2.83	18	12	**0.035**	0.304	–	–	–	–		1.64	20	27	0.115	
NEE	0.68	18	13	0.777		2.25	20	28	**0.024**	0.126	–	–	–	–	

Bold values represent *p* values ≤0.05

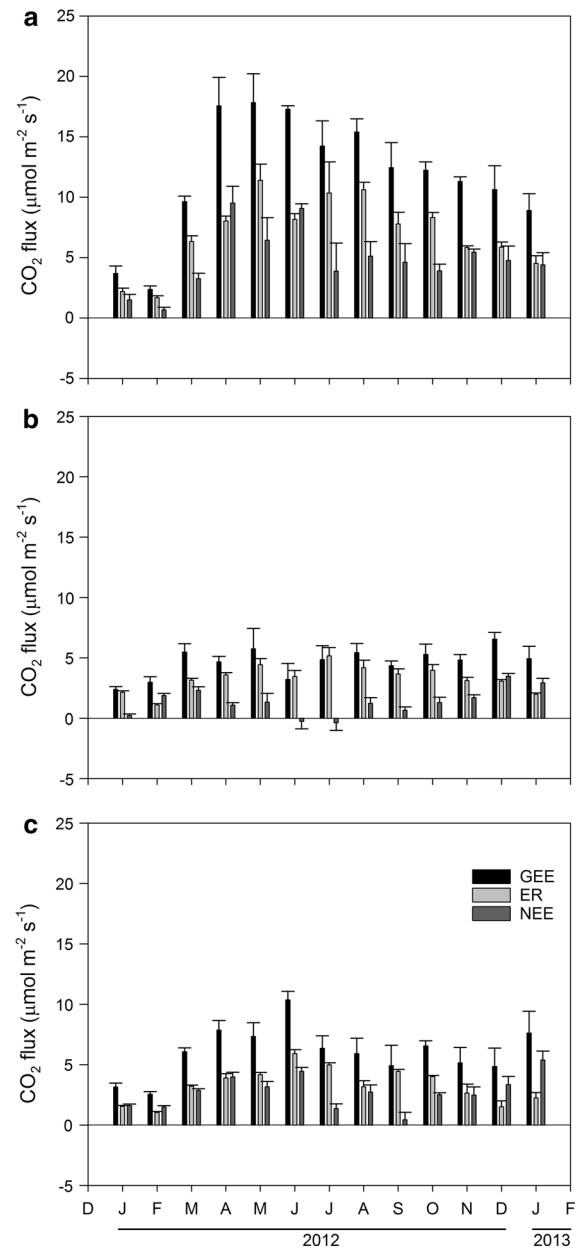

Fig. 5 Midday gross ecosystem exchange (GEE), ecosystem respiration of CO_2 (ER_{CO2}), and net ecosystem exchange (NEE) for Week's Bay (**a**) Dog River (**b**) and Dauphin Island (**c**) plotted for each month at each site ($n = 3$). NEE was measured at maximum light intensity ± 2 h of solar noon. A positive NEE value indicates a net flux of C from the atmosphere into the marsh, whereas negative values are the reverse. *Error bars* represent ± 1 SD

$p = 0.170$) to each other, with the exception of April ($p = 0.022$) and June 2012 ($p < 0.001$), in which GEE at Dauphin Island was slightly higher.

Monthly integrations

Monthly-integrated GEE at all sites peaked in spring and early summer 2012 (April–June) and then declined steadily through the fall and winter months (Fig. 6). GEE ranged from a peak at Week's Bay during April (185.1 g C m^{-2} mo^{-1}) to a low during February (13.7 g C m^{-2} mo^{-1}). GEE at Dog River had minimal annual variation (18.0 to 54.0 g C m^{-2} mo^{-1}, February and July, respectively). Monthly-integrated GEE was highest at Week's Bay for 9 out of 13 months ($F_{(24,70)} = 7.32, p < 0.001$) while there were only minimal differences in GEE between Dauphin Island and Dog River during the spring growing season when rates were slightly greater at Dauphin Island (Fig. 6). While GEE at both Week's Bay and Dauphin Island exhibited some seasonality, GEE at Dog River showed minor seasonality with consistently lower rates occurring over the entire year. Monthly-integrated GEE fluxes were significantly different between Dog River and Dauphin Island ($F_{(1,38)} = 9.10, p = 0.004$), with more C being fixed at Dauphin Island during the growing season. Integrated over the 2012 study year, GEE was 1210.5 ± 72.5, 513.7 ± 43.7, and 655.6 ± 44.6 g C m^{-2} $year^{-1}$ at Week's Bay, Dog River, and Dauphin Island, respectively.

Monthly-integrated ER_{CO2} had the greatest range at Week's Bay with a maximum of 276.1 g C m^{-2} mo^{-1} in July and a minimum of 93.5 g C m^{-2} mo^{-1} in November 2012 (Fig. 6). There was very minor monthly variation in ER_{CO2} between Dog River and Dauphin Island, which ranged from 56.8 to 119.5 and 50.8 to 134.6 g C m^{-2} mo^{-1}, respectively. ER_{CO2} was higher at Week's Bay compared to Dog River and Dauphin Island (Tukey's, $q = 4.99, p < 0.001$), while there was no difference in rates between Dog River and Dauphin Island (Tukey's, $q = 0.83, p = 0.832$). Within each site, ER_{CO2} was positively correlated to soil temperature but not to any of the other variables tested (Table 3). Similar to monthly-integrated GEE, ER_{CO2} was nearly identical at Dog River and Dauphin Island and followed each other well throughout the entire study period. Annual ER_{CO2} was 2103.9 ± 115.4, 1031.5 ± 41.5, and 1065.8 ± 53.6 g C m^{-2} $year^{-1}$ for Week's Bay, Dog River, and Dauphin Island, respectively.

Estimated NEE varied both temporally and spatially across all sites, but unlike midday NEE, it suggested

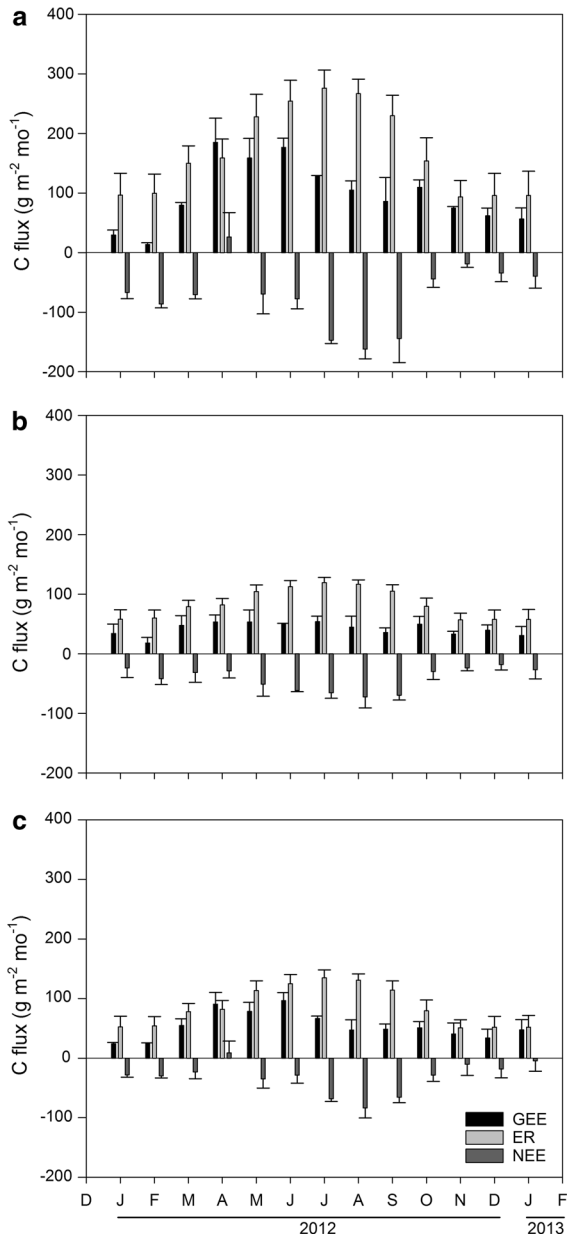

Fig. 6 Monthly-integrated rates of GEE, ER_{CO2}, and NEE for Week's Bay (**a**) Dog River (**b**) and Dauphin Island (**c**) calculated from respiration versus temperature and light response relationships combined with environmental data recorded during each sampling day. *Error bars* represent ± 1 SD of *triplicate plots*

that all sites are C sources to the atmosphere for a majority of the study period (Fig. 6). The only sites acting as minor C sinks during the 2012 year were Week's Bay (26.2 g C m^{-2} mo^{-1}) and Dauphin Island (8.6 g C m^{-2} mo^{-1}) during April. Dog River was a

Table 4 Results from the warming simulation showing changes in ER_{CO2} when subjected to a 2 and 4 °C temperature increase versus current temperatures

	ER_{CO_2} (g CO_2 m^{-2} $year^{-1}$)		
	Current	2 °C	4 °C
Week's Bay	2103.9	2497.2	2964.2
Dog River	1031.5	1156.8	1297.2
Dauphin Island	1065.8	1242.0	1447.3

CO_2 source to the atmosphere over the entire study period. NEE varied most at Week's Bay and ranged from −162.0 to 26.2 g C m^{-2} mo^{-1}. NEE showed a strong C source signal during the late summer (July–*September* 2012) when GEE was declining but ER was just reaching its maximum (Fig. 6). Mean NEE was negative across all sites, indicating that each marsh was a net source of CO_2 to the atmosphere. Annually-integrated NEE was greatest at Week's Bay (−893.4 ± 187.9 g C m^{-2} $year^{-1}$) and decreased as salinity increased, with slightly less C emitted at Dog River (−517.8 ± 85.2 g C m^{-2} $year^{-1}$) and Dauphin Island (−410.2 ± 98.2 g C m^{-2} $year^{-1}$). There was a difference in NEE across sites for the entirety of the study period ($F_{(2,12)} = 12.97$, $p = <0.001$). Week's Bay was the greatest CO_2 source to the atmosphere while there was no difference between Dog River and Dauphin Island (Holm-Sidak, $t = 1.22$, $p = 0.232$).

Warming simulation

When subjected to a temperature increase, ER_{CO2} at all sites experienced an increase in CO_2 loss (Table 4). With a 2 °C temperature increase, response was greatest at Week's Bay and Dauphin Island (18.7 and 16.5 % increase, respectively) while the response at Dog River was lower (12.1 % increase). At a 4 °C increase, response was once again greatest at Week's Bay and Dauphin Island (40.9 and 35.8 % increase, respectively), while ER_{CO2} at Dog River only increased by 25.8 %.

Porewater analyses

Depth-integrated inventories (0–25 cm) of dissolved CH_4 in sediment porewaters exhibited a seasonal pattern of lower concentrations in the winter and spring seasons (61.8 ± 12.6 μmol m^{-2}, April 2012, Week's Bay) and higher concentrations in the autumn months (7551 ± 1004 μmol m^{-2}, November 2012, Dauphin Island; Fig. 7a). Throughout all of the months sampled and contrary to expectations, CH_4 inventories at Dauphin Island were 70–115 % higher than at Dog River and Week's Bay, respectively ($t = 3.55$, $p = 0.004$). There was no difference in CH_4 inventories between Dog River and Week's Bay ($t = 1.46$, $p = 0.159$). Peak porewater CH_4 concentrations were greatest at Dauphin Island (449 μM), followed by Dog River (364 μM) and Week's Bay (259 μM; Fig. 8). Contour plots (Fig. 8) revealed porewater CH_4 built up in the sediments in late summer (August) and peaked in autumn (*September*–November).

Depth-integrated inventories (0–25 cm) of porewater H_2S exhibited a similar seasonality as dissolved porewater CH_4. Inventories were typically low during the winter months, steadily increasing during the spring months, and peaking in late summer (Fig. 7b). Inventories were always lowest at Week's Bay, and had a monthly average of 398.0 ± 189.4 μmol m^{-2}. Over the entire study period, average porewater H_2S inventories were similar between Dog River and Dauphin Island ($t = 2.04$, $p = 0.102$).

SO_4^{2-} depletion values represent the net result of SO_4^{2-} production from oxidation of sulfides and SO_4^{2-} removal by microbial reduction. Depth-integrated (to 20 cm) SD ranged from −335 ± 86 mmol m^{-2} (Week's Bay, January 2013) to 1114 ± 227 mmol m^{-2} (Dauphin Island, July 2012) and was negative (excess SO_4^{2-}) only during the winter months (February and December 2012, January 2013), while porewaters at all sites were depleted in SO_4^{2-} spring through autumn (Fig. 9). SD at Dauphin Island was significantly higher than Week's Bay (Tukey's, $q = 4.04$, $p < 0.05$) but was not significantly different than Dog River (Tukey's, $q = 1.16$, $p > 0.05$). SD at Week's Bay and Dog River were similar throughout the study period (Tukey's, $q = 2.89$, $p > 0.05$).

Discussion

Counter to our expectations, all marshes were a net CO_2 source over the study period, and there was little difference in the magnitude of CH_4 fluxes across the

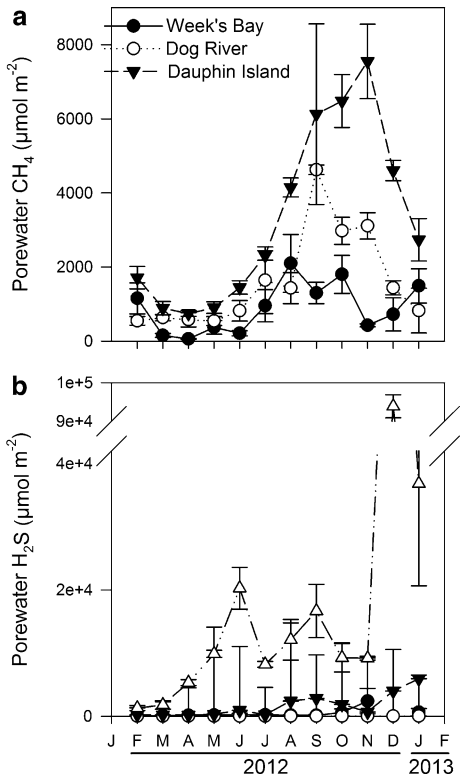

Fig. 7 Depth-integrated inventories (0–25 cm) of dissolved porewater CH_4 (**a**) and H_2S (**b**). *Error bars* represent the SD of the mean of triplicate measurements

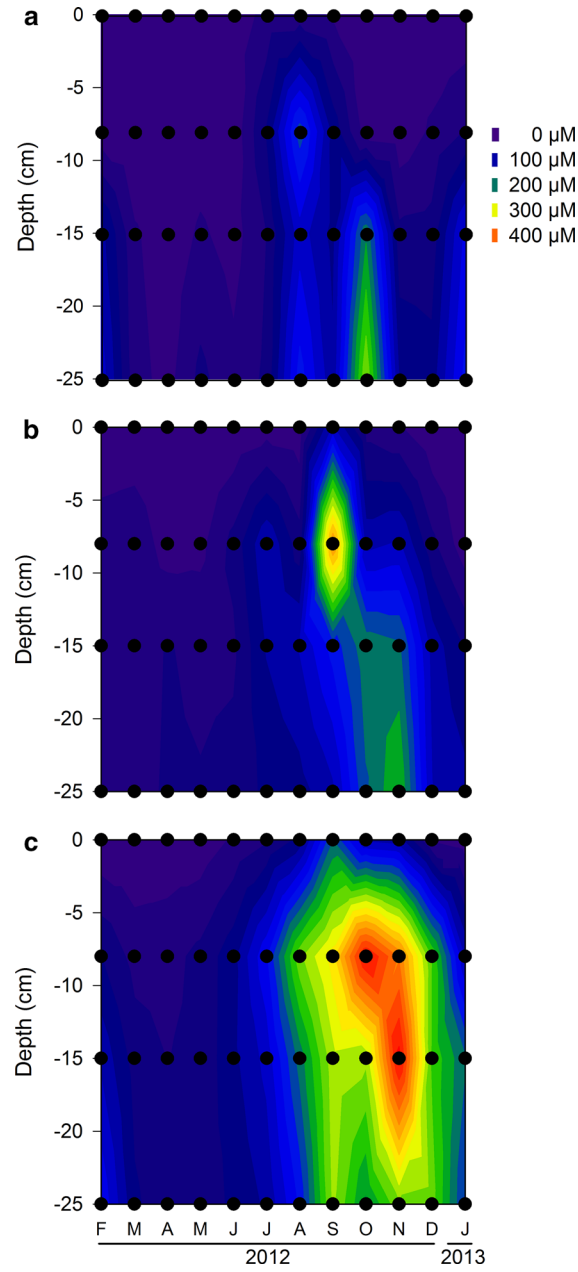

Fig. 8 Contour plots showing changes in porewater CH_4 concentrations from Week's Bay (**a**) Dog River (**b**) and Dauphin Island (**c**) over the course of the study period. Samples, indicated by *black dots*, were taken in triplicate at each site per month down to 25 cm depth

salinity gradient. Surprisingly, porewater CH_4 inventories were highest at the salt marsh. Below, we discuss some of the particular controls that could be influencing C fluxes from these marshes and conclude with discussion about what effects a changing climate may have on the perseverance of northern Gulf of Mexico coastal marshes.

Primary production in Mobile Bay marshes

Maximum midday GEE was 68–104 % higher at Week's Bay compared to Dog River with the most significant differences occurring from the onset of the growing season until the end of the year (March–December 2012; Fig. 5). The highest C assimilation occurred at Week's Bay because of very high GEE during the spring growing season when soil temperatures were still low and ER_{CO2} was minimal. These differences in midday GEE were observed despite no differences in vegetation type or live aboveground biomass between Week's Bay and Dog River (Table 1), suggesting that some belowground process must be limiting GEE at Dog River. Throughout the study period, porewater sulfide inventories were 50–316 % higher at Dog River compared to Week's Bay (Fig. 7b). Increases in metabolic

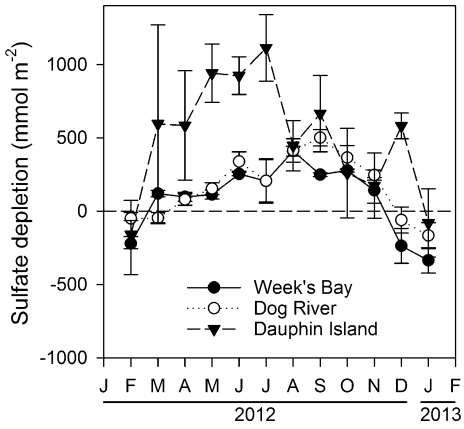

Fig. 9 Depth-integrated SO_4^{2-} depletion (SD) at each site. SO_4^{2-} depletion is calculated from measured porewater SO_4^{2-} and chloride concentrations: SD = $[Cl^-] \times 0.0517 - [SO_4^{2-}]$. Positive SD values indicate net consumption by SO_4^{2-} reduction whereas negative values indicate net accumulation of SO_4^{2-}. *Error bars* represent the SD of *triplicate plots*

products, such as sulfide, with higher salinities can stress wetland plants and decrease productivity (Koch et al. 1990; Munns and Tester 2008). High sulfide concentrations can also have a potentially toxic effect on plant roots. During times of stress, wetland plants use their flow-through aerenchyma to provide a rapid flow of oxygen to their root tissues growing in anaerobic sediments (Armstrong 1979; Seago et al. 2005). Some typical freshwater wetland plants, however, have a reduced capacity to provide oxygen to their roots in times of saltwater intrusion (Pahl 2002). Indeed, *C. jamaicense*, the dominant plant species at Week's Bay and Dog River, is less efficient at internal aeration in times of strongly reducing conditions (Chabbi et al. 2000). Less internal aeration can lead to areas of oxygen deficiency in the rhizosphere and induce alcoholic fermentation, producing potentially toxic ethanol that can severely inhibit GEE (Chabbi et al. 2000; Crawford 1967; Delaune et al. 1983b). Sulfide concentrations of up to 120 μM were measured in sediment porewaters at Dog River compared to 20 μM at Week's Bay, which is sufficient to inhibit GEE (Ingold and Havill 1985; Koch et al. 1990). Similarly, high sulfide concentrations (202–1264 μM) most likely contributed to Dauphin Island having 40–90 % lower maximum GEE compared to Week's Bay, although other factors such as lower aboveground biomass, different vegetation type, and hydroperiod (flooded every high tide) likely contributed as well.

Carbon losses from Mobile Bay marshes

Higher salinity and lower GEE at Dauphin Island may have led ER_{CO2} to be 72 % lower compared to Week's Bay (Fig. 5) as ER_{CO2} and GEE are tightly linked (Cannell and Thornley 2000). While we do not have a direct measurement of SO_4^{2-} reduction rates, porewater SO_4^{2-} and sulfide concentrations indicate high rates of SO_4^{2-} reduction may be contributing significantly to ER_{CO2} at Dauphin Island. In salt marsh sediments, both SO_4^{2-} and iron reduction generally dominate anaerobic metabolism while other processes, such as denitrification and methanogenesis account for only a small portion (Howarth and Teal 1979; Miley and Kiene 2004; Senior et al. 1982; Tobias and Neubauer 2009). Howes et al. (1984) showed in a *S. alterniflora* marsh that the primary source of CO_2 production below 2 cm originated from organic matter mineralization via SO_4^{2-} reduction. Sediment porewaters at Dauphin Island were depleted in SO_4^{2-} relative to seawater concentrations for a majority of the year, especially during the spring through fall seasons, indicating that SO_4^{2-} reduction occurred at a greater rate than sulfide oxidation or diffusion from overlying seawater for most of that time (Fig. 9). *S. alterniflora* sediments, however, do not benefit from large radial oxygen loss from the roots and maintain an oxygenated zone limited to the root-water interface (Koretsky et al. 2003, 2008). Low oxygen diffusion from the roots into the sediments may allow for SO_4^{2-} reduction to be an important pathway of microbial respiration for a majority of the year at the Dauphin Island marsh.

Mean daily CH_4 flux was higher at Week's Bay (28.8 mg C m^{-2} day^{-1}) compared to Dog River and Dauphin Island (14.4 and 15.6 mg C m^{-2} day^{-1}, respectively), though this difference was not statistically significant. Several previous studies have established relationships predicting CH_4 flux based on porewater salinity. According to previously published salinity relationships, one would expect an average of 16.8 (Bartlett et al. 1987) and 14.4 times (Poffenbarger et al. 2011) more CH_4 emissions at Week's Bay (salinity of 3.8) compared to Dauphin Island (salinity of 24.5). Similarly, one would expect 14.1 and 12.2 times greater CH_4 efflux from Dog River (5.1 ppt)

compared to Dauphin Island; however, CH_4 fluxes at Week's Bay were only 1.9 times greater while there was little difference between Dog River and Dauphin Island. Predicting CH_4 flux based solely on porewater salinity (Poffenbarger et al. 2011) may lead to both overestimates and underestimates of fluxes.

Lower than expected CH_4 efflux based on porewater salinity and high dissolved porewater CH_4 concentrations suggest that a significant quantity of CH_4 oxidation occurs at the sediment-atmosphere interface (Fig. 8). Up to 52–81 % of diffusive CH_4 fluxes were oxidized and converted to CO_2 in a tidal freshwater swamp (Megonigal and Schlesinger 2002). Kelley et al. (1995) found a tenfold discrepancy in CH_4 production compared to measured CH_4 flux and attributed the difference to bacterially mediated CH_4 oxidation near the sediment surface during low tide. Low measured CH_4 effluxes at our sites could be influenced by hydrology. Because all fluxes were measured at low or neap tide, surficial sediments were exposed to the atmosphere, potentially allowing oxygen to diffuse into the sediments and stimulate methanotrophic bacteria (Chmura et al. 2011; Whalen 2005). As H_2S was always detected in porewater sippers at 10 cm depth, this was a good indicator that subsurface sediments remained anoxic. Therefore, favorable reduced conditions persisted in the sediments, and it was likely that most CH_4 was oxidized near the sediment surface. Alternatively, episodic ebullition events could have resulted in emitted CH_4 to the atmosphere (Goodrich et al. 2011), or tidal flooding could have transported dissolved CH_4 from the marsh (Tong et al. 2010), both of which were unaccounted for.

Net ecosystem exchange and tidal marsh accretion

While midday NEE indicated C uptake by all three sites (Fig. 5), monthly-integrated NEE fluxes showed all sites as a net C source to the atmosphere, with no difference in the rates across sites (Fig. 6). Because NEE flux was measured on mostly sunny days, these monthly-integrated NEE fluxes indicate a best possible net C uptake scenario in which little to no cloud cover would reduce PAR. Therefore, the result that all three sites were net C sources to the atmosphere over the course of the month was unexpected. Coastal marshes can sequester between 1.5 and 142.8 g C m^{-2} mo^{-1} (McLeod et al. 2011). However, results from our study indicate that these coastal marshes lost 34.2–74.5 g CO_2 m^{-2} mo^{-1} with minimal change in magnitude along a salinity gradient (Table 5).

One possible explanation for the measured C losses during this study is that GEE and ER_{CO2} might be out of phase, meaning that C accumulated one year may not be decomposed and respired until the following year leading to a temporal imbalance between these two processes (Falge et al. 2002; Neubauer et al. 2000). A comparison of January 2012 and January 2013 shows a negative NEE one year and a neutral to positive NEE the next (Fig. 6c). It is possible that the system may be under a stressor (e.g. temperature, salinity) in early 2012 that would cause the marshes to respire more C rather than incorporating it (Larcher 2003). For example, unusually high temperatures during January 2012 (21.6 °C) compared to January 2013 (11.8 °C) may have contributed to higher ER_{CO2} at Week's Bay and Dauphin Island. Standing litter in marshes can also have a negative impact on light reaching the vegetation and therefore influence NEE (Knapp and Seastedt 1986; Rocha et al. 2008). Although we do not have seasonal estimates of aboveground biomass, a one-time assessment revealed that a substantial proportion of total aboveground biomass at all three sites in this study was standing litter (Table 1), which has been shown to reduce NEE in marshes by 17–47 % (Rocha et al. 2008).

Seasonal exposure to saltwater can also inhibit NEE. Although we do not have continuous measurements of salinity at each site, in our monthly discrete samples, we did see salinity become elevated in both the porewaters and surface waters during some months (November and December; Fig. 3). This saltwater intrusion could depress plant productivity and increase organic matter remineralization, ultimately leading to greater C losses (Neubauer 2013; Weston et al. 2011). *Cladium*, the dominant macrophyte at both Week's Bay and Dog River, is predominately a freshwater plant with some marginal ability to tolerate salinity. Macek and Rejmankova (2007) found that *Cladium* plant height and root to shoot biomass decreased with simulated saltwater intrusion, while others have shown that *Cladium* aboveground net primary production decreases as salinity increases, with slow recovery after exposure to high levels of salinity (Childers et al. 2006). Weston et al. (2014) found that an oligohaline marsh in the Delaware River Estuary was not accumulating any C as a result of seasonal

saltwater intrusion. It is possible that these marshes are in a state of transition from freshwater and oligohaline to mesohaline marshes or possibly even non-vegetative mudflats depending on whether or not they are able to accrete at the rate of relative SLR. While there are many possibilities why these marshes showed net C efflux to the atmosphere, further interannual NEE measurements are needed before any conclusion can be made.

In order for tidal marshes to accrete at the same rate as current SLR, vegetative growth and sedimentation inputs must occur at a greater rate than organic matter breakdown and sedimentation outputs (i.e. erosion) (Kirwan and Megonigal 2013). The finding of positive NEE (C efflux) from these marshes runs counter to other gas flux studies from coastal wetlands (Miller et al. 2001; Neubauer 2013), which could imply that some fraction of the sediment is being mineralized and lost from the marsh (Neubauer et al. 2002). Without an additional subsidy, the marsh may be in danger of succumbing to SLR in the long-term.

Wetland plants have been shown to have a strong influence on sedimentation as they can baffle the flow of water containing suspended sediments, causing particles to settle and increase sedimentation (Silva et al. 2009; Yang 1999). This sedimentation can play two roles in marsh accretion. First, deposition of particulate organic C during tidal flooding can counterbalance C lost through respiration and allow marshes to keep a positive balance with respect to C (net sink). Neubauer et al. (2000) found a freshwater tidal marsh in Virginia to be a net C source through CO_2 and CH_4 emissions (-207 g C m^{-2} $year^{-1}$). However, when sediment deposition (as organic C) was taken into account, 517 g C m^{-2} $year^{-1}$ was deposited on the marsh, accounting for C lost through respiratory processes and providing sufficient input to allow for vertical accretion to keep pace with SLR (Neubauer et al. 2002).

Another potential reason why we saw overall C losses from these marshes is that organic C delivered via sedimentation would stimulate microbial respiration and enhance ER_{CO2}. Much of this added organic matter could have come from strong coastal storms, such as tropical storms and hurricanes. Coastal storms can deposit large quantities of sediments and add elevation to coastal marshes as well as potentially affecting the ecosystem C balance (Baumann et al. 1984; Stone et al. 1997; Tweel and Turner 2012). Immediately prior to our study in 2011, and during our study in August 2012, Tropical Storm Lee and Hurricane Isaac indirectly affected the study area with elevated storm surge and extended periods of inundation ($\sim$1–2 weeks). Although we did not measure sedimentation rates, these two storms most likely deposited inorganic and organic material on the marsh surface. High ER_{CO2} seen at all three marshes may be the result of decomposition of this material.

Inorganic sedimentation from tidal flooding and freshwater runoff is crucial for marsh accretion against SLR (Kirwan and Megonigal 2013). Within the Mobile Bay estuary, sediment cores indicate that sediment accumulation at coastal marshes along both the east and west banks has been largely driven by large, episodic inputs of inorganic material, which can account for more than 90 % of net mass accumulation at the marsh (Smith et al. 2013). For example, on the northern Gulf of Mexico coast west of the current study area, Hurricanes Katrina and Rita deposited between 3 and 13 cm of sediment (Horton et al. 2009; McKee and Cherry 2009; Turner et al. 2006). Coastal storms strike the northern Gulf of Mexico coast on average once every 3 years (Keim and Muller 2007). This frequency and type of episodic deposition could have many important impacts, including changing the vegetation type in an area and affecting the C balance through additions of organic and inorganic material.

Sedimentation within the Mobile Bay watershed has been greatly altered and reduced as a result of human activities (Roach et al. 1987), and sedimentation during normal tidal flooding and freshwater river runoff may not provide the marsh with enough deposition to keep pace with SLR (Morris et al. 2002; Stevenson et al. 1988). Coastal Alabama wetlands have been disappearing at an alarming rate, with 50 % lost over a 200-year period from 1780 to 1980 (Dahl 1990). Even more recently, Alabama lost 29 % of its nonfresh marshes between 1955 and 1979 (Roach et al. 1987), much higher than the national average loss of 8 % (Frayer et al. 1983). Unsurprisingly, human activities, such as development and water channel manipulation, has accounted for an estimated 48 % of the coastal Alabama marsh loss, yet $\sim$47 % can be attributed to natural processes such as erosion, subsidence and natural succession (Roach et al. 1987). Net C loss at our sites can destabilize marshes through organic matter

breakdown, potentially leading to subsidence and peat collapse (Delaune et al. 1994), a process that might have contributed to the marsh loss in Alabama.

Future implications

The future fate of coastal marshes will be influenced by climate change, as increased rates of SLR will cause saltwater to intrude more into coastal marshes. Much emphasis has recently been placed on attempting to discern how each of these factors will affect marsh C cycling with both positive and negative impacts possible (reviewed in Kirwan and Megonigal 2013). Negative feedbacks could reduce productivity as a result of increased respiration from warmer temperatures (Kirwan and Blum 2011) and higher salinity from increased saltwater intrusion (Neubauer 2013; Rasse et al. 2005). Results from our warming simulation show a 12–41 % increase in ER_{CO2} depending on how much temperatures rise over the next century (Table 4). Such increases in respiratory losses of C could potentially destabilize marshes. Increased temperature associated with increased radiative forcing can increase plant growth by 10–40 % as a result of longer growing seasons (Kirwan et al. 2009), but this is unlikely to occur in northern Gulf of Mexico marshes where extending an already long growing season may have little effect, and some vegetation, such as *S. alterniflora*, is already photosynthesizing at its optimal temperature during the growing season (Giurgevich and Dunn 1979; Kirwan et al. 2009). In our study, marshes were respiring more C than they were accumulating, and this further stresses the importance that inorganic and organic sedimentation will play on coastal marsh survival in the future (Turner et al. 2006). Regardless of the process or mechanism, tidal marshes must accrete at the same rate as SLR or risk permanent inundation. While most studies have simply looked at vertical accretion rates (Chmura et al. 2003), gas flux studies show coastal marshes can be both C sources (this study, Neubauer et al. 2000; Weston et al. 2014) and sinks (Kathilankal et al. 2008; Neubauer 2013; Weston et al. 2014). Future gas flux studies coupled with sedimentation rate measurements are needed to determine the future response of tidal marshes within northern Gulf of Mexico estuaries to climate change and anthropogenic impacts.

Table 5 Average rates of annually integrated net ecosystem exchange (NEE), gross ecosystem exchange (GEE), and ecosystem CO_2 respiration (ER_{CO2}) for each site

Flux (g m^{-2} yr^{-1})	Week's Bay	Dog River	Dauphin Island
NEE	−893.4 ± 187.9	−517.8 ± 85.2	−410.2 ± 98.2
GEE	1210.5 ± 72.5	513.7 ± 43.7	655.6 ± 44.6
ER_{CO2}	2103.9 ± 115.4	1031.5 ± 41.5	1065.8 ± 53.6

The SD reflects the variability across plots ($n = 3$)

Conclusions

Although plant composition and sedimentary processes in coastal marshes typically change as a function of salinity, overall NEE did not vary significantly with salinity at marsh sites in Mobile Bay, on the northern Gulf of Mexico. Porewater salinity, which ranged from 1.9 to 26.9 ppt, was not a significant driver of ER_{CH4} from these sites, and ER_{CH4} did not vary across the salinity gradient. Surprisingly, each marsh was found to be a net CO_2 source over the entire study period. This finding runs counter to recent global estimates of C burial rates by salt marshes (218 ± 24 g C m^{-2} $year^{-1}$; McLeod et al. 2011). Our study indicates that Gulf of Mexico marshes may be vulnerable to SLR due to net C losses, especially with increased respiration rates in a warming climate over the next century. Further work is needed to determine if processes such as inorganic and organic sedimentation can offset C losses and allow these marshes to keep pace with SLR.

Acknowledgments B. Wilson was supported by a University of Alabama Biological Sciences Graduate Teaching Assistantship. We thank all of the DISL technical and support staff for funding vehicle use and nutrient analysis. We would like to thank Christina Staudhammer for statistical assistance, Greg Starr and Karina Schafer for providing reviews of previous manuscript drafts, and S. Neubauer whose advice and comments greatly improved this manuscript. We would also like to thank Jennifer Anders, Rebecca Bernard, and Alice Kleinhuizen for help in the field and the lab.

References

Armstrong W (1979) Aeration in higher plants. In: Woolhouse H (ed) Advances in botanical research. Academic Press, London, pp 225–332

Bartlett KB, Bartlett DS, Harriss RC, Sebacher DI (1987) Methane emissions along a salt-marsh salinity gradient. Biogeochemistry 4(3):183–202

Bastviken D, Tranvik LJ, Downing JA, Crill PM, Enrich-Prast A (2011) Freshwater methane emissions offset the continental carbon sink. Science 331(6013):50

Baumann RH, Day JW, Miller CA (1984) Mississippi deltaic wetland survival: sedimentation versus coastal submergence. Science 224(4653):1093–1095

Bridgham SD, Megonigal JP, Keller JK, Bliss NB, Trettin C (2006) The carbon balance of North American wetlands. Wetlands 26(4):889–916

Cannell M, Thornley J (2000) Modelling the components of plant respiration: some guiding principles. Ann Bot 85:45–54

Chabbi A, McKee KL, Mendelssohn IA (2000) Fate of oxygen losses from *Typha domingensis* (Typhaceae) and *Cladium jamaicense* (Cyperaceae) and consequences for root metabolism. Am J Bot 87(8):1081–1090

Childers DL, Iwaniec D, Rondeau D, Rubio G, Verdon E, Madden CJ (2006) Responses of sawgrass and spikerush to variation in hydrologic drivers and salinity in Southern Everglades marshes. Hydrobiologia 569:273–292

Chmura GL, Anisfeld SC, Cahoon DR, Lynch JC (2003) Global carbon sequestration in tidal, saline wetland soils. Global Biogeochem Cycles 17(4):12

Chmura GL, Kellman L, Guntenspergen GR (2011) The greenhouse gas flux and potential global warming feedbacks of a northern macrotidal and microtidal salt marsh. Environ Res Lett 6(4):44016

Crawford RM (1967) Alcohol dehydrogenase activity in relation to flooding tolerance in roots. J Exp Bot 18(56):458–464

Dahl T (1990) Wetlands losses in the United States, 1780′s to 1980′s. In: Chipley R, Flack S (eds) US fish and wildlife service report to congress. Chelsea House, Washington, p 13

Delaune RD, Smith CJ, Patrick WH (1983a) Methane release from gulf-coast wetlands. Tellus B 35(1):8–15

Delaune RD, Smith CJ, Patrick WH (1983b) Relationship of marsh elevation, redox potential, and sulfide to *Spartina alterniflora* productivity. Soil Sci Soc Am J 47(5):930–935

Delaune RD, Nyman JA, Patrick WH (1994) Peat collapse, pending and wetland loss in a rapidly submerging coastal marsh. J Coast Res 10(4):1021–1030

Duarte CM, Middelburg JJ, Caraco N (2005) Major role of marine vegetation on the oceanic carbon cycle. Biogeosciences 2(1):1–8

Falge E, Baldocchi D, Tenhunen J, Aubinet M, Bakwin P, Berbigier P, Bernhofer C, Burba G, Clement R, Davis KJ, Elbers JA, Goldstein AH, Grelle A, Granier A, Guomundsson J, Hollinger D, Kowalski AS, Katul G, Law BE, Malhi Y, Meyers T, Monson RK, Munger JW, Oechel W, Paw KT, Pilegaard K, Rannik U, Rebmann C, Suyker A, Valentini R, Wilson K, Wofsy S (2002) Seasonality of ecosystem respiration and gross primary production as derived from FLUXNET measurements. Agric For Meteorol 113(1–4):53–74

Fonselius S (1976) Determination of hydrogen sulphide. In: Grasshoff K (ed) Methods of seawater analysis. Verlag Chemie, Weinheim, pp 71–78

Frayer W, Monahan J, Bowden D, Graybill F (1983) Status and trends of wetlands and deepwater habitats in the conterminous United States: 1950s to 1970s. In: Hook DD, Crawford RMM (eds) Department of forest and wood sciences. Colorado State University, Fort collins

Giurgevich JR, Dunn EL (1979) Seasonal patterns of CO_2 and water-vapor exchange of the tall and short height forms of *Spartina alterniflora* loisel in a Georgia salt marsh. Oecologia 43(2):139–156

Goodrich JPGJP, Varner RK, Frolking S, Duncan BN, Crill PM (2011) High-frequency measurements of methane ebullition over a growing season at a temperate peatland site. Geophys Res Lett 38:1–5

Horton BP, Rossi V, Hawkes AD (2009) The sedimentary record of the 2005 hurricane season from the Mississippi and Alabama coastlines. Quat Int 195:15–30

Howarth RW, Teal JM (1979) Sulfate reduction in a New England salt marsh. Limnol Oceanogr 24(6):999–1013

Howes BL, Dacey JWH, King GM (1984) Carbon flow through oxygen and sulfate reduction pathways in salt marsh sediments. Limnol Oceanogr 29(5):1037–1051

Hsieh YP, Yang CH (1997) Pyrite accumulation and sulfate depletion as affected by root distribution in a *Juncus* (needle rush) salt marsh. Estuaries 20(3):640–645

Inglett KS, Inglett PW, Reddy KR, Osborne TZ (2012) Temperature sensitivity of greenhouse gas production in wetland soils of different vegetation. Biogeochemistry 108(1–3):77–90

Ingold A, Havill DC (1985) Some effects of sulfide invitro on selected enzymes, oxygen-uptake and ion-uptake in 4 salt marsh plant species. Comp Physiol Ecol 10(1):1–6

IPCC (2007) Contribution of working group I to the fourth assessment report of the intergovernmental panel on climate change. Cambridge University Press, Cambridge

Kathilankal JC, Mozdzer TJ, Fuentes JD, D'Odorico P, McGlathery KJ, Zieman JC (2008) Tidal influences on carbon assimilation by a salt marsh. Environ Res Lett 3(4):044010

Keim BD, Muller RA (2007) Spatiotemporal patterns and return periods of tropical storm and hurricane strikes from Texas to Maine. J Clim 20(14):3498–3509

Kelley CA, Martens CS, Ussler W (1995) Methane dynamics across a tidally flooded riverbank margin. Limnol Oceanogr 40(6):1112–1129

Kirwan ML, Blum LK (2011) Enhanced decomposition offsets enhanced productivity and soil carbon accumulation in coastal wetlands responding to climate change. Biogeosciences 8(4):987–993

Kirwan ML, Megonigal JP (2013) Tidal wetland stability in the face of human impacts and sea-level rise. Nature 504(7478):53–60

Kirwan ML, Guntenspergen GR, Morris JT (2009) Latitudinal trends in *Spartina alterniflora* productivity and the response of coastal marshes to global change. Glob Change Biol 15(8):1982–1989

Knapp AK, Seastedt TR (1986) Detritus accumulation limits productivity of tallgrass prairie. Bioscience 36(10):662–668

Koch MS, Mendelssohn IA, McKee KL (1990) Mechanism for the hydrogen sulfide-induced growth limitation in wetland macrophytes. Limnol Oceanogr 35(2):399–408

Koretsky CM, Moore CM, Lowe KL, Meile C, Dichristina TJ, Van Cappellen P (2003) Seasonal oscillation of microbial

iron and sulfate reduction in saltmarsh sediments (Sapelo Island, GA, USA). Biogeochemistry 64(2):179–203
Koretsky CM, Haveman M, Cuellar A, Beuving L, Shattuck T, Wagner M (2008) Influence of *Spartina* and *Juncus* on saltmarsh sediments I. pore water geochemistry. Chem Geol 255(1–2):87–99
Larcher W (2003) Physiological plant ecology. Springer, Berlin
Macek P, Rejmankova E (2007) Response of emergent macrophytes to experimental nutrient and salinity additions. Funct Ecol 21(3):478–488
Magenheimer JF, Moore TR, Chmura GL, Daoust RJ (1996) Methane and carbon dioxide flux from a macrotidal salt marsh, Bay of Fundy New Brunswick. Estuaries 19(1):139–145
McKee KL, Cherry JA (2009) Hurricane Katrina sediment slowed elevation loss in subsiding brackish marshes of the Mississippi River delta. Wetlands 29(1):2–15
McLatchey GP, Reddy KR (1998) Regulation of organic matter decomposition and nutrient release in a wetland soil. J Environ Qual 27(5):1268–1274
McLeod E, Chmura GL, Bouillon S, Salm R, Bjork M, Duarte CM, Lovelock CE, Schlesinger WH, Silliman BR (2011) A blueprint for blue carbon: toward an improved understanding of the role of vegetated coastal habitats in sequestering CO_2. Front Ecol Environ 9(10):552–560
Megonigal JP, Schlesinger WH (2002) Methane-limited methanotrophy in tidal freshwater swamps. Glob Biogeochem Cycles 16(4):35–41
Miley GA, Kiene RP (2004) Sulfate reduction and porewater chemistry in a gulf coast *Juncus roemerianus* (Needlerush) marsh. Estuaries 27(3):472–481
Miller WD, Neubauer SC, Anderson IC (2001) Effects of sea level induced disturbances on high salt marsh metabolism. Estuaries 24(3):357–367
Morris JT, Sundareshwar PV, Nietch CT, Kjerfve B, Cahoon DR (2002) Responses of coastal wetlands to rising sea level. Ecology 83(10):2869–2877
Munns R, Tester M (2008) Mechanisms of salinity tolerance. Annu Rev Plant Biol 59:651–681
Neubauer SC (2013) Ecosystem responses of a tidal freshwater marsh experiencing saltwater intrusion and altered hydrology. Estuar Coasts 36(3):491–507
Neubauer SC, Miller WD, Anderson IC (2000) Carbon cycling in a tidal freshwater marsh ecosystem: a carbon gas flux study. Mar Ecol-Prog Ser 199:13–30
Neubauer SC, Anderson IC, Constantine JA, Kuehl SA (2002) Sediment deposition and accretion in a mid-Atlantic (USA) tidal freshwater marsh. Estuar Coast Shelf Sci 54(4):713–727
Neubauer SC, Givler K, Valentine SK, Megonigal JP (2005) Seasonal patterns and plant-mediated controls of subsurface wetland biogeochemistry. Ecology 86(12):3334–3344
Page SE, Rieley JO, Banks CJ (2011) Global and regional importance of the tropical peatland carbon pool. Glob Change Biol 17(2):798–818
Pahl J (2002) The combined effects of salinity and sulfide on the growth and physiology of the freshwater marsh plant *Panicum hemitomon* J.A. Schultes. Louisiana State University, Baton Roug
Perry JE, Hershner CH (1999) Temporal changes in the vegetation pattern in a tidal freshwater marsh. Wetlands 19(1):90–99
Pezeshki SR, Delaune RD, Patrick WH (1987) Effects of flooding and salinity on photosynthesis of *Sagittaria lancifolia*. Mar Ecol Prog Ser 41(1):87–91
Poffenbarger HJ, Needelman BA, Megonigal JP (2011) Salinity influence on methane emissions from tidal marshes. Wetlands 31(5):831–842
Rasse DP, Peresta G, Drake BG (2005) Seventeen years of elevated CO_2 exposure in a Chesapeake Bay wetland: sustained but contrasting responses of plant growth and CO_2 uptake. Glob Change Biol 11(3):369–377
Reddy KR, DeLaune RD (2008) Biogeochemistry of wetlands: science and applications. CRC Press, Boca Raton
Roach E, Watzin M, Scurry J, Johnston J (1987) Wetland changes in coastal Alabama. In: Lowery T (ed) Symposium on the national resources of the Mobile Bay estuary. Alabama Sea Grant Extension Service, Mobile, pp 92–101
Rocha AV, Potts DL, Goulden ML (2008) Standing litter as a driver of interannual CO_2 exchange variability in a freshwater marsh. J Geophys Res Biogeosci 113:1–16
Schuyler AE, Andersen SB, Kolaga VJ (1993) Plant zonation changes in the tidal portion of the Delaware River. Proc Acad Natl Sci Phila 144:263–266
Seago JL, Marsh LC, Stevens KJ, Soukup A, Votrubova O, Enstone DE (2005) A re-examination of the root cortex in wetland flowering plants with respect to aerenchyma. Ann Bot 96(4):565–579
Senior E, Lindstrom EB, Banat IM, Nedwell DB (1982) Sulfate reduction and methanogenesis in the sediment of a saltmarsh on the east coast of the United Kingdom. Appl Environ Microbiol 43(5):987–996
Silva H, Dias JM, Cacador I (2009) Is the salt marsh vegetation a determining factor in the sedimentation processes? Hydrobiologia 621:33–47
Smith CG, Osterman LE, Poore RZ (2013) An examination of historical inorganic sedimentation and organic matter accumulation in several marsh types within the Mobile Bay and Mobile-Tensaw River delta region. J Coast Res 63:68–83
Stevenson JC, Ward LG, Kearney MS (1988) Sediment transport and trapping in marsh systems-implications of tidal flux studies. Mar Geol 80(1–2):37–59
Stone GW, Grymes JM, Dingler JR, Pepper DA (1997) Overview and significance of hurricanes on the Louisiana coast USA. J Coast Res 13(3):656–669
Symbula M, Day FP (1988) Evaluation of 2 methods for estimating belowground production in a fresh-water swamp forest. Am Midl Nat 120(2):405–450
Tobias CR, Neubauer SC (2009) Salt marsh biogeochemistry–an overview. In: Cahoon D, Perillo G, Wolansky E, Brinson M (eds) Coastal wetlands: an integrated ecosystem approach. Elsevier Press, Amsterdam, pp 445–492
Tong C, Wang WQ, Zeng CS, Marrs R (2010) Methane (CH_4) emission from a tidal marsh in the Min River estuary, southeast China. J Environ Sci Health Part A 45(4):506–516
Turner RE, Baustian JJ, Swenson EM, Spicer JS (2006) Wetland sedimentation from Hurricanes Katrina and Rita. Science 314(5798):449–452
Tweel AW, Turner RE (2012) Landscape-scale analysis of wetland sediment deposition from four tropical cyclone events. Plos One 7(11):e50528

Vourlitis GL, Oechel WC, Hastings SJ, Jenkins MA (1993) A system for measuring insitu CO_2 and CH_4 flux in unmanaged ecosystems: an arctic example. Funct Ecol 7(3):369–379

Weston NB, Dixon RE, Joye SB (2006) Ramifications of increased salinity in tidal freshwater sediments: geochemistry and microbial pathways of organic matter mineralization. J Geophys Res-Biogeosci. doi:10.1029/2005JG000071

Weston NB, Vile MA, Neubauer SC, Velinsky DJ (2011) Accelerated microbial organic matter mineralization following salt-water intrusion into tidal freshwater marsh soils. Biogeochemistry 102(1–3):135–151

Weston NB, Neubauer SC, Velinsky DJ, Vile MA (2014) Net ecosystem carbon exchange and the greenhouse gas balance of tidal marshes along an estuarine salinity gradient. Biogeochemistry 120:163–189

Whalen SC (2005) Biogeochemistry of methane exchange between natural wetlands and the atmosphere. Environ Eng Sci 22(1):73–94

Whiting GJ, Bartlett DS, Fan SM, Bakwin PS, Wofsy SC (1992) Biosphere atmosphere CO_2 exchange in tundra ecosystems: community characteristics and relationships with multispectral surface reflectance. J Geophys Res Atmos 97(D15):16671–16680

Yang SL (1999) Sedimentation on a growing intertidal island in the Yangtze River mouth. Estuar Coast Shelf Sci 49(3):401–410